Structural Engineering and Mechanics, Vol. 36, No. 1 (2010) 95-110
DOI: http://dx.doi.org/10.12989/sem.2010.36.1.095

Using multiple point constraints in finite element analysis of two dimensional contact problems

*C.H. Liu[1], I Cheng[1], An-Chi Tsai[1], Lo-Jung Wang[2] and J.Y. Hsu[3]

[1]*Department of Mechanical and Elector-mechanical Engineering, Tamkang University, Tamsui, Taipei Shien, Taiwan, R.O.C.*
[2]*UL International Services Ltd.-Taiwan Branch, 1'st Fl 260 Da-Yeh Road, Peitou, Taipei City, Taiwan, R.O.C.*
[3]*Vivotek Inc., 6F 192 Lien-Cheng Rd., Chung-Ho, Taipei Shien, Taiwan, R.O.C.*

(Received August 14, 2008, Accepted May 6, 2010)

Abstract. Two-dimensional elastic contact problems, including normal, tangential, and rolling contacts, are treated with the finite element method in this study. Stress boundary conditions and kinematic conditions are transformed into multiple point constraints for nodal displacements in the finite element method. Upon imposing these constraints into the finite element system equations, the calculated nodal stresses and nodal displacements satisfy stress and displacement contact conditions exactly. Frictional and frictionless contacts between elastically identical as well as elastically dissimilar materials are treated in this study. The contact lengths, sizes of slip and stick regions, the normal and the shear stresses can be found.

Keywords: contact mechanics; rolling contact; tangential contact; finite element method; multiple point constraints.

1. Introduction

Contact stress analysis plays an important role in designing mechanical components such as bearings, gears and pinions, cams and followers, and wheel and rail. A contact problem can be characterized as static (or quasi-static) if accelerations are negligible; otherwise it is dynamic. A static contact problem may be further characterized as a case of *normal contact* when tangential resultant force is absent, or as a case of *tangential contact* when tangential forces exist. Likewise, when two or more bodies are in *rolling contact*, the motion is called *steady rolling* when material particles "flow through" the contact region with a steady-state motion. If tangential tractions are transmitted in the contact region, the phenomenon is called *tractive rolling*. A normal contact problem determines the size of the contact region and the normal pressure in the region. In both tangential and rolling contact problems, the unknowns are the normal pressure, the size of the contact zone, and the tangential tractions in the contact zone, hence the normal contact can be considered as a part of the tangential and the rolling contact problems. Also, in a case of tractive

*Corresponding author, Professor, E-mail: chaohwa@mail.tku.edu.tw

rolling, local sliding, also called slipping, always occurs; hence a method that solves rolling contact problems can also deal with normal and tangential contacts. In this study the normal contact, the tangential contact, and the rolling contact problems are treated, but the emphasis is placed on steady rolling between two elastic bodies.

Contact problems may be formulated by the following two methods: nonlinear variational principles, and integral equations (Knothe *et al.* 2001). Nonlinear variational formulation of normal contact problems generally involves variational inequalities (Duvaut and Lions 1976, Wriggers 2006, Kikuchi and Oden 1988, Eterovic and Bathe 1991, Buscaglia *et al.* 2001, Hassani *et al.* 2003, Solberg and Papadopoulos 2005, Mohamed *et al.* 2006, Solberg *et al.* 2007, Ferronato 2008), and these inequality constraints may be imposed upon the finite element procedure by various methods (Wriggers 2006). The most complete variational formulation for rolling contact, within the domain of linear elasticity, is due to Kalker (1990); his formulation is based on complementary energy principles. Formulations for visco-elastic rolling solids have also been derived (Duvaut and Lions 1976, Padovan and Paramadilok 1984, Tallec and Rahier 1994). These rolling contact formulations may be conveniently expressed in the arbitrary Lagrange Eulerian (ALE) description (Wriggers 2006, Nackenhorst 2004).

Integral equation formulation of rolling contact problems may date from 1926 when Carter (1926) obtained an analytical solution for the tangential stress of two rolling cylinders. Up to now numerical solutions still check against his results. Johnson (1958a) obtained kinematic relations during rolling contact [Eq. (9) below, see also Kalker 1967)]. Johnson (1958b) also obtained approximate solutions for a sphere rolling on a plane. Liu and Paul (1989) utilized fundamental solutions obtained by Cerruti (1882) to turn the kinematic equations obtained by Johnson (1958a) into integral equations for tangential stresses, and they obtained numerical solutions for cases with small spins. By simplifying the rail by a series of springs, Kalker (1973, 1991) was able to obtain approximate solutions for wheel-rail rolling contact. Gonzalez and Abascal (1998) developed a boundary element method for rolling contact between dissimilar materials. Kakoi and Obara (1993) developed a special boundary element technique to deal with rolling contacts of counterformal bodies. Pauk and Zastrau (2003) analyzed two-dimensional rolling contact problems with a boundary element technique; surface roughness was taken into consideration during their analysis. Semi-analytical solutions of integral equations were obtained for various types of contacts, for example, Ozsahin (2007) obtained solutions for frictionless contact of a layer on an elastic half plane, Nowell *et al.* (1988b) obtained solutions for two-dimensional normal and tangential contacts (see also Hills *et al.* 1993), Nowell and Hills (1988a) obtained solutions for rolling contact.

Between the above-mentioned two major formulations for rolling contact problems, the integral equations formulation is mathematically straightforward. Both stresses and displacements may be used as principal unknowns and hence both stress and displacement boundary conditions can be satisfied exactly at each node. But this formulation utilizes fundamental solutions, which are still unknown for many nonlinear material responses. Even for problems with linear elastic materials, fundamental solutions for a finite domain with a concave boundary are not generally available (Paul and Hashemi 1981). In contrast to the integral equation formulation, formulations based upon nonlinear variational principles can deal with bodies with various shapes and have various kinds of nonlinear responses. Special contact elements based on the nonlinear variational principles have been developed and incorporated into commercial finite element software. But in the assumed-displacement finite element formulation the variables are nodal displacements and nodal forces, stress boundary conditions can not be directly imposed. Also, nonlinear variational principles involves sophisticated mathematics, hence are understood only by experts. To many practicing engineers contact elements based on nonlinear variational principles are used without the understanding of its theory.

There are a few attempts to combine the two above-mentioned formulations. Wang *et al.* (2005) proposed a direct constraint hybrid Trefftz finite element method for frictionless normal contact problems. Interfacial force equilibrium is ensured by the constraint conditions. González *et al.* (2008) showed that a finite element mesh may be in contact with a boundary element mesh, by inserting a contact frame between them. They utilized variational formulation in the analysis. Earlier Liu and Hsu (2000) proposed the idea to transform stress boundary conditions into multiple constraints for nodal displacements. They only considered normal contact problems and treated two cases with elastically identical materials. Their constraint equations had obvious errors that caused inaccurate results in the case of frictional contact. The method to use extrapolated stresses through multiple point constraints was not pursued further; until now in the present study we show that, with the correct constraint equations, the method can be used to solve normal, rolling, and tangential contacts with or without friction and between similar or dissimilar materials. In this study both stress boundary conditions and kinematic conditions are transformed into multiple point constraints for nodal displacements, and upon incorporating these linear constraints into the finite element system equations, the nodal displacements and nodal stresses satisfy the kinematic conditions and stress boundary conditions exactly. Compared to the two major formulations mentioned above, this method is a finite element technique, but without using nonlinear variational principles, also without using any special contact element. The method also resembles the integral equation formulation since stress boundary conditions are satisfied exactly by the extrapolated nodal stresses; but no fundamental solutions are required.

2. Contact boundary conditions

Fig. 1 shows an illustrative mesh of two bodies before contact. If nodes j and k will be in contact, then their displacements v in the y direction satisfy the relation

$$v_j - v_k = h(x) \tag{1}$$

where $h(x)$ is the gap distance before contact. The two nodes have the same normal and shear stresses, i.e.

$$(\sigma_{yy})_j = (\sigma_{yy})_k \tag{2}$$

$$(\tau_{xy})_j = (\tau_{xy})_k \tag{3}$$

The above three conditions are satisfied by every pair of nodes in the contact zone. If the two nodes are in the slip region, meaning that relative slip occurs at these nodes, then according to Coulomb's law of friction

$$(\tau_{xy})_j = \mu(\sigma_{yy})_j \tag{4}$$

where μ is the coefficient of friction. If this pair of nodes is in the stick region, then kinematic conditions must be used, as discussed below.

Assuming two equal and opposite tangential forces Q are applied to two elastic bodies already in

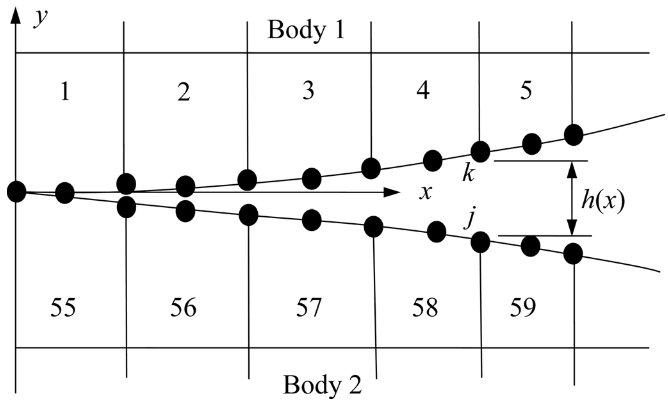

Fig. 1 An illustrative mesh of two bodies before contact

contact, then the tangential displacement of node j relative to node k, denoted by S_x, is given by (Johnson 1985, p.210-212)

$$S_x = \delta_x + (u_j - u_k) \tag{5}$$

where u_j and u_k are nodal displacements in the x (i.e., tangential) direction, δ_x is the tangential displacement of a point on body 2, which is far away from the contact region, relative to a point on body 1, which is also far away from the contact region. The displacement δ_x may be called *rigid displacement*, since it is the relative displacement for every remote pair of points on the two bodies. Note that δ_x is positive when body 2 is moving towards the right with respect to body 1. If nodes j and k are in the stick region, then $S_x = 0$ and the kinematic equation takes the form

$$\delta_x + (u_j - u_k) = 0 \tag{6}$$

The previous equation holds for a pair of nodes in the stick region during tangential contact. In the special case of normal contact, the rigid displacement δ_x is zero, Eq. (5) becomes

$$S_x = u_j - u_k \tag{7}$$

which reduces to the form

$$u_j - u_k = 0 \tag{8}$$

when the two nodes are in the stick region. The kinematic equation for rolling contact is described below.

Fig. 2 shows the upper body (body 1) rolls over the lower body (body 2) with a counterclockwise instantaneous angular velocity. At the instant body 1 is subjected to a counterclockwise couple, traction $(\tau_{xy})_1$ on body 1 develops in the contact region to balance this couple, and $(\tau_{xy})_2$ is its equal but opposite counterpart on body 2. In a rolling contact problem relative motion is expressed by *relative velocity*, without the possibility of confusion, let the notation S_x also denote the relative tangential velocity of two originally coinciding nodes j and k in rolling contact, then this relative speed is given by Johnson (1958a, see also Johnson 1985, pp. 242-245) as follows

$$S_x = \xi_x + (\partial u/\partial x)_j - (\partial u/\partial x)_k \tag{9}$$

where ξ_x is called *creep ratio*; the meaning of this parameter can be illustrated by considering

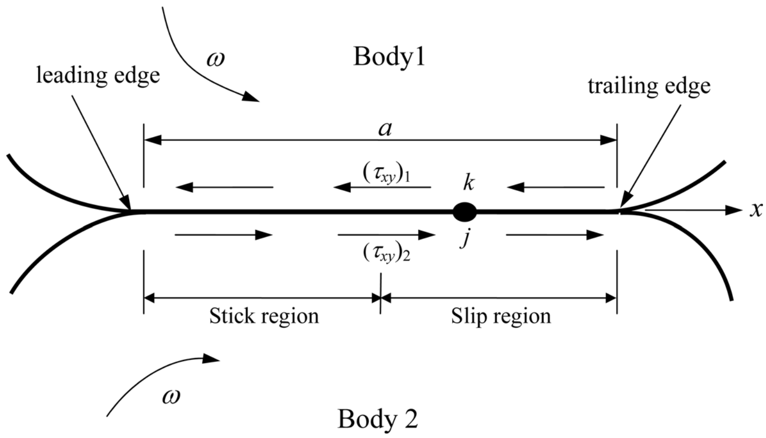

Fig. 2 Two bodies in rolling contact

bodies 1 and 2 as two rolling cylinders of radii r_1 and r_2 respectively, and these two cylinders originally have the same average circumferential speed V, namely $V = r_1\omega_1 = r_2\omega_2$, before tractions $(\tau_{xy})_1$ and $(\tau_{xy})_2$ occur in the contact region. But as tangential tractions develop, elastic deformation due to these tractions changes the circumferences of two cylinders, making average circumferential speed of these two cylinders differ, and ξ_x is a parameter to represent this difference. It is the speed increment of body 1 subtracts from the speed increment of body 2, and then dividing this difference by the original speed V to make it dimensionless.

If both nodes j and k are in the stick region, which is generally located at the leading edge when contact is between two identical materials as Fig. 2 shows, then there is no relative speed between these two nodes, i.e., $S_x = 0$ and Eq. (9) becomes

$$\xi_x + (\partial u/\partial x)_j - (\partial u/\partial x)_k = 0 \tag{10}$$

In this study all forces are assumed to be monotonically increasing and stresses are assumed to be increased in proportional, so that stresses do not depend on loading history.

3. Multiple point constraints

Eqs. (1), (6), and (8) are called multiple point constraints for nodal displacements, since each of them involves displacements at more than one node. Other equations, namely Eqs. (2), (3), (4), and (10), are now to be transformed into multiple point constraints for nodal displacements.

In the finite element method nodal stresses may be accurately calculated by extrapolating stresses at Gaussian points, and these Gaussian stresses are given by

$$\boldsymbol{\sigma}_i = \mathbf{B}(\xi_i, \eta_i)\mathbf{d} \tag{11}$$

where (ξ_i, η_i) are coordinates of the i'th Gaussian integration point in the isoparametric ξ-η plane, $\boldsymbol{\sigma}_i = [\sigma_{xx} \ \ \sigma_{yy} \ \ \tau_{xy}]^T$ is the stress vector at the i'th Gaussian integration point, $\mathbf{B}$ is the strain matrix, and $\mathbf{d}$ is the element nodal displacement vector. In this study all analyses are performed with eight-node quadratic isoparametric elements using 3×3 Gaussian integration. To extrapolate Gaussian stresses to a node, say node j, one may establish another isoparametric coordinate system s-t such that $(s,t) = (\xi, \eta)/\sqrt{0.6}$ (see Cook *et al.* 2001, p.231-232, for this extrapolation). Then the stress vector at the j'th node may be expressed as

$$\boldsymbol{\sigma}_j = \sum_{i=1}^{9} N_i(s_j, t_j)\boldsymbol{\sigma}_i \tag{12}$$

where N_i are shape functions for nine-node quadratic isoparametric elements, and (s_j, t_j) denotes coordinates of the j'th node in the s-t coordinate system. Substituting Eq. (12) into Eq. (11), also making use of stress-strain relations, one may obtain the nodal stress vector at the j'th node in element n, as follows

$$(\boldsymbol{\sigma}_j)_n = \mathbf{E}^n \sum_{i=1}^{9} N_i(s_j, t_j)\mathbf{B}(\xi_i, \eta_i)\mathbf{d}_n \tag{13}$$

where subscript/superscript n denotes that the variable is defined for element n, $\mathbf{E}^n$ is material constant matrix for element n. The condition that the j'th node of element n and the k'th node of element m have the same stress σ_{yy} [i.e., Eq. (2)] may be expressed in the form

$$\mathbf{E}_2^n \sum_{i=1}^{9} N_i(s_j, t_j)\mathbf{B}(\xi_i, \eta_i)\mathbf{d}_n = \mathbf{E}_2^m \sum_{i=1}^{9} N_i(s_k, t_k)\mathbf{B}(\xi_i, \eta_i)\mathbf{d}_m \tag{14}$$

where $\mathbf{E}_2^n$ and $\mathbf{E}_2^m$ are row vectors that contain only the second rows of the material constant matrices $\mathbf{E}^n$ and $\mathbf{E}^m$, respectively. Only the second rows are needed since σ_{yy} appears in the second row of the stress vector. The extrapolated nodal stresses are discontinuous across the element boundary, hence generally the equal stress condition [i.e., Eq. (2)] is written twice for a boundary node. For example, if the j'th node of element n is a boundary node and is also a node of element $n+1$, and the k'th node of element m is also a node of element $k+1$, then, in addition to equation (14), the equal stress condition should be written again for elements $n+1$ and $k+1$ as well. Another situation is the j'th node of element n is a boundary node but the k'th node of element m is not, then the average stress of the former node equals to the stress of the latter node.

If the shear stresses at nodes j and k are equal [i.e., Eq. (3)], then the corresponding multiple point constraint is

$$\mathbf{E}_3^n \sum_{i=1}^{9} N_i(s_j, t_j)\mathbf{B}(\xi_i, \eta_i)\mathbf{d}_n = \mathbf{E}_3^m \sum_{i=1}^{9} N_i(s_k, t_k)\mathbf{B}(\xi_i, \eta_i)\mathbf{d}_m \tag{15}$$

Eq. (4) can be treated in a similar way, giving rise to the following result

$$\mathbf{E}_3^n \sum_{i=1}^{9} N_i(s_j, t_j)\mathbf{B}(\xi_i, \eta_i)\mathbf{d}_n = \mu \mathbf{E}_2^n \sum_{i=1}^{9} N_i(s_j, t_j)\mathbf{B}(\xi_i, \eta_i)\mathbf{d}_n \tag{16}$$

and finally, Eq. (9) relates two normal strains ε_{xx} at nodes j and k; it can be transformed into the following form

$$\xi_x + \sum_{i=1}^{9} N_i(s_j, t_j)\mathbf{B}_1(\xi_i, \eta_i)\mathbf{d}_n - \sum_{i=1}^{9} N_i(s_k, t_k)\mathbf{B}_1(\xi_i, \eta_i)\mathbf{d}_m = 0 \tag{17}$$

where $\mathbf{B}_1$ is the row vector which contains only the first row of the strain matrix $\mathbf{B}$.

Eq. (16) couple the 16 nodal displacements in the vector $\mathbf{d}_n$, and Eqs. (14), (15), and (17) couple the 32 displacements in vectors $\mathbf{d}_n$, and $\mathbf{d}_m$. Whenever node j and node k are in contact, Eqs. (1), (14), and (15) are always valid at this pair of nodes. If nodes j and k are in the slip region, then equation (16) is also imposed, but if these two nodes are in the stick region, then, depending on the nature of the problem (i.e., normal, tangential, or rolling contact), one of the three Eqs. (6), (8), or (17) is imposed as well. The 3×3 Gaussian integration rule should be used in the finite element procedure, as Eqs. (14)-(17) shows, since the 2×2 integration rule does not gives rise to correct results, i.e., when the 2×2 integration rule is used in Eqs. (14)-(17), and also in the finite element procedure to calculate stiffness matrices and to perform stress extrapolation, then the nodal stresses so obtained do not satisfy Eqs. (2)-(4) (Hsu 1998); this phenomenon requires further studies.

As a check of solutions, the tangential traction in the stick region should be less than its limiting value, namely

$$|\tau_{xy}|_j < \mu|\sigma_{yy}|_j \tag{18}$$

Furthermore, when solutions are obtained, relative slip S_x can be found from Eq. (5), Eq. (7), or Eq. (9), depending on the nature of the problem. Since the tangential stress τ_{xy} always opposes the relative slip S_x, the calculated S_x and τ_{xy} should satisfy the following relation at any node in the slip region,

$$\tau_{xy}/|\tau_{xy}| = -S_x/|S_x| \tag{19}$$

Eqs. (18) and (19) are used to check solutions.

4. Analysis procedure

Contact stress analysis can be classified into the *forward analysis* and the *inverse analysis*. In the forward analysis the applied forces are given, the contact length and the normal as well as tangential contact stresses in the contact region are to be determined. In the inverse analysis the rigid displacements, the creep ratio, and sometimes even the contact length are assumed before the analysis. Contact stresses are determined in the analysis and the corresponding applied forces are obtained by integrating the stresses over the contact region. The forward analysis generally involves iterations on the size of the contact region and also adjustments of mesh sizes. The inverse analysis generally is simpler for one execution, but to obtain contact stresses caused a given force, a complete force-displacement curve should be generated by a series of executions. Then the rigid displacement corresponding to this force is obtained from the force-displacement curve, and is used as the input to another analysis to obtain contact stresses. Hence in an inverse analysis many executions are needed for one specified force. Both the forward and the inverse analyses can be carried out by the finite element method, but the integral equation formulation can only be implemented with the inverse analysis. The purpose of this article is to present the idea of using multiple point constraints. The inverse analysis is adopted in this study to avoid tedious iterations on the contact length and mesh adjustments. The number of elements in contact is assumed a priori, and the rigid displacement δ_x in a case of tangential contact, or the creep ratio ξ_x in a case of rolling contact, is the input parameter. The numerical procedure solves for the corresponding normal force P, the tangential force Q, and the normal/tangential stress distribution in the contact region. Two-dimensional contacts between two cylinders, as shown in Fig. 3, are treated, and procedures for normal contact problems are discussed first.

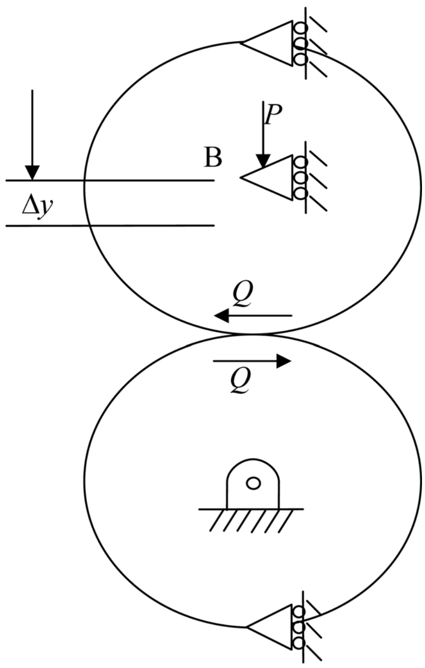

Fig. 3 Two cylinders in contact

4.1 Procedures for normal contact analysis

The purpose for a normal contact analysis is to determine the prescribed displacement Δy see Fig. 3 that produces a specified contact length $2a$, as well as the normal stress in the contact region. When the contact is with friction, the tangential stress and sizes of both the stick and the slip regions are also to be found. The prescribed displacement Δy eliminates the upper cylinder's remaining rigid body motion that was not suppressed by supports. Procedures for a frictional normal contact analysis are given below.

1. Assume at the outset that the stick region extends to the whole contact zone, thus multiple point constraints (1), (8), (14), and (15) are imposed on every node pair.
2. Adjust the prescribed displacement Δy, until the following two conditions are satisfied:
   i) Nodal stress σ_{yy} is compressive at every node inside the contact region.
   ii) $\sigma_{yy} \approx 0$ at the outermost node on either side of the contact region.
3. Check if tangential stress τ_{xy} exceeds its limiting value $\mu\sigma_{yy}$ at every node pair in the stick region. If condition (18) is violated at a particular node pair, then in the next analysis, slip is assumed to occur at this node pair, on which multiple point constraints (1), (14), (15), and (16) are imposed. Note that condition (16) should be applied to both nodes.
4. The previous step (step 3) alters the stresses in the slip region, which is generally located next to the contact boundary. Hence the stress σ_{yy} at the outermost boundary may be affected by step 3, and one should repeat step 2.
5. Repeat step 3, and then go back to step 2 again. Until all conditions specified in steps 2 and 3 are satisfied.
6. The normal force P required to produce the specified contact region is the reaction force at the

node of prescribed displacement Δy.

4.2 Procedures for rolling contact analysis

The normal contact analysis should always be performed prior to a rolling contact analysis to obtain the prescribed displacement Δy corresponding to a specified contact length $2a$. In a case of rolling contact between two cylinders made of different materials, an accelerating moment given to the upper cylinder (body 1) causes tangential stress to develop in the contact region, and if the upper cylinder is softer than the lower, this accelerating moment also produces an apparent increase in the magnitude of the compressive stress σ_{yy} at the trailing edge (Hills *et al.* 1993, Nowell and Hills 1988a); implying that the contact length extends to the right. In this study we specify the increment in the number of contact elements at the trailing edge prior to the analysis, and determine the corresponding tangential force and creep ratio to produce such an increase of contact length; the normal and tangential stresses, as well as sizes of the stick and the slip regions, are also determined. Numerical procedures given below are for the situation that an accelerating moment is given to the upper cylinder, which is softer than the other.

1. Assume that initially the whole contact region is stick, and multiple point constraints (1), (14), (15), and (17) are imposed for every node pair in the contact region.
2. Determine the tangential force Q, and the corresponding creep ratio ξ_x. This step is an iterative procedure in itself, explained as follows:
   i) Perform the finite element analysis with an arbitrarily assumed creep ratio ξ_x, and an arbitrarily assumed value of the tangential force Q.
   The tangential force Q may be distributed evenly to each node on the upper body in the contact region, and the equal but opposite force $-Q$ is also distributed evenly to the counterpart nodes on the lower body. For the case with an accelerating moment given to the upper cylinder which is also the softer one, $\xi_x < 0$, and the direction of the force pair $\pm Q$ is the same as shown in Fig. 3.
   ii) Adjust values of ξ_x and Q so that $\sigma_{yy} \approx 0$ at both the leading and the trailing edges. The following tendencies can be observed while adjusting these values.
   An increase of the force Q causes the contact region to shift to the right, in other words, at the leading it causes a decrease in the magnitude of the compressive stress σ_{yy}, and at the trailing edge an increase. Also, an increase in $|\xi_x|$ (ξ_x<0) causes an increase in contact length at both ends; i.e., it increases the magnitudes of compressive stress σ_{yy} at both edges. Therefore, if σ_{yy} is negative (positive) at both ends, then one should decrease (increase) the value of $|\xi_x|$ in the next iteration, and if σ_{yy} is negative (positive) at the left end and is positive (negative) at the right end, then one should increase (decrease) the value of Q in the next iteration. The changes in ξ_x or Q decrease rapidly, until they are negligible.
3. If tangential stress τ_{xy} exceeds its limiting value $\mu\sigma_{yy}$ at a particular node pair, then in the next analysis this pair is considered to be in the slip region upon which multiple point constraints (1), (14), (15), and (16) are imposed.
4. Repeat step 2; only minor adjustments of ξ_x and Q are needed.
5. Repeat step 3, and then repeat step 2 again, until all conditions of steps 2 and 3 are satisfied.

The relative slip S_x can be calculated from Eq. (9) and one should check if Eq. (19) is valid at every node in the slip region. The direction of friction should be reversed wherever Eq. (19) is not valid, and this can be done by reversing the sign of coefficient of friction in Eq. (16).

4.3 Procedures for tangential contact analysis

The procedures for tangential contact analysis of two cylinders of dissimilar materials are essentially the same as the previous steps for rolling contact, except that the creep ratio is replaced by the rigid displacement δ_x, and that Eq. (6) instead of Eq. (17) is used in the stick region. The two tendencies mentioned in step 2 are still valid, if the creep ratio is replaced by the displacement δ_x.

4.4 Cylinders of identical materials

Analysis becomes much simpler in a case of rolling contact between two cylinders with elastically identical materials, since in this case both the contact pressure and the contact length obtained by the normal contact analysis are unaffected by the presence of tangential stress (Johnson 1985, pp. 202-204). The purpose of a rolling contact analysis is to determine the tangential force Q corresponds to a given creep ratio ξ_x, when the contact region and contact pressure are already obtained from a normal contact analysis. While all other steps remain the same, the second step of the rolling contact procedure in section 4.2 can be greatly simplified, and is modified as follows.

Step 2. For a given creep ratio ξ_x, determine the tangential force Q such that $\tau_{xy} \approx 0$ at the leading edge. As in the case of dissimilar materials, a value of the tangential force Q can be arbitrarily assumed, and both Q and $-Q$ are distributed evenly to contacting nodes on the upper and the lower bodies, respectively. Adjust the value of Q, until $\tau_{xy} \approx 0$.

5. Results and discussions

To carry out the above-mentioned numerical technique, the finite element program has to be able to treat multiple constraints with 32 nodal displacements, and to have eight-node quadratic isoparametric elements using the 3×3 Gaussian integration in the linear elastic analysis. There may be commercial programs capable of performing the above-mentioned procedures; nevertheless the authors developed a program written in MATLAB to perform finite element calculations. Finite element mesh is generated with ANSYS. Multiple point constraints are treated by the technique of Lagrange multipliers (see for example Hedayatr *et al.* 2007), which generally gives accurate results at the cost of an increase in system bandwidth. Both cylinders shown in Fig. 3 are stable, thus the original stiffness matrix is positive definite; meaning that a Gaussian elimination process can solve the system equations (Cook *et al.* 2001, p.492). The technique of Lagrange multipliers increases number of equations, but the authors solve the system equations with the built-in function of MATLAB that deals with sparse matrices.

Contact meshes shown in Fig. 4 and in Fig. 5 are for cases with identical and with dissimilar materials, respectively. In a case with dissimilar materials, the contact length is affected by the magnitude of the tangential force; thus for the convenience of adjusting contact length, the layout shown in Fig. 5 has finer meshes at the both ends. In cases of identical materials, the complete mesh contains 384 elements and 1258 nodes, and in cases of dissimilar materials, there are 436 elements and 1418 nodes.

In all examples that follow, the two cylinders have the same radius of 100 mm. Materials are steel and aluminum whose moduli of elasticity $E = 210$ Gpa and 70 Gpa, and Poisson's ratios $\upsilon = 0.28$ and 0.33 respectively. The coefficients of friction are $\mu = 0.22$ and $\mu = 0.13514$ for cases with

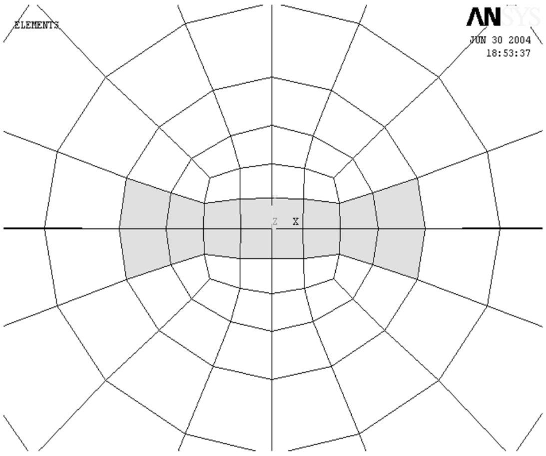

Fig. 4 Elements in the contact region for elastically identical materials

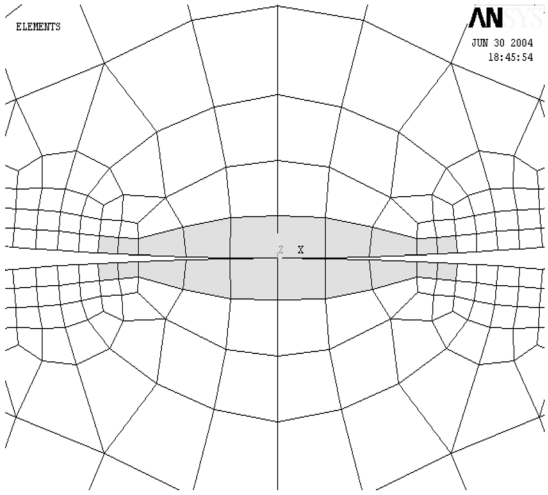

Fig. 5 Element in the contact region; dissimilar materials

identical and with dissimilar materials, respectively. The iterative procedures suggested above are empirical; the authors are unable to prove the convergence. However, in this study all iterative procedures converged. For normal contact analysis, convergence is achieved within 8 adjustments of Δy if tolerance for σ_{yy} at the boundary is 0.01% of the peak pressure. For rolling or tangential contacts of dissimilar materials, the procedure for adjusting ξ_x (or δ_x) may converge in 5 iterations but we used a larger tolerance for σ_{yy}, that is, 0.1% of the peak pressure.

Fig. 6 shows results for a frictionless normal contact between elastic identical materials, and they are compared with the Hertzian contact pressure. As the contact half-width $a = 0.17815$ mm, the calculated normal force P is 29.24 N, which is close to the Hertzian value $P = 28.39$ N.

Figs. 7 and 8 show normal and shear stresses for two elastic identical materials under rolling contact, compared to Hertz's and to Carter's (1926) results, respectively. Carter's result for shear stress is given by

$$\tau_{xy} = \mu p_0[\sqrt{1-(x/a)} - (c/a)\sqrt{1-(x+d)^2/c^2}] \tag{20}$$

where a is the contact half-length, c is half-length of the stick region, $d = a - c$, and p_0 is the peak pressure at the center $x = 0$. Results shown in Figs. 7 and 8 reveal that normal stresses are accurately calculated and the tangential stress in the stick region is slightly higher. In Fig. 9 the relation between the creep ratio ξ_x and the tangential force Q is compared to the following analytical solution (Johnson 1985, p.253)

$$\xi_n = -\mu a(1-\sqrt{1-Q/\mu P})/R \tag{21}$$

where R is one half of the radius of the two cylinders. Fig. 9 shows the present solutions agree well with the last equation. More results for elastically identical materials can be found in Tsai (2004).

The following are cases of dissimilar cylinders in frictional contact. Body 1 and body 2 are made

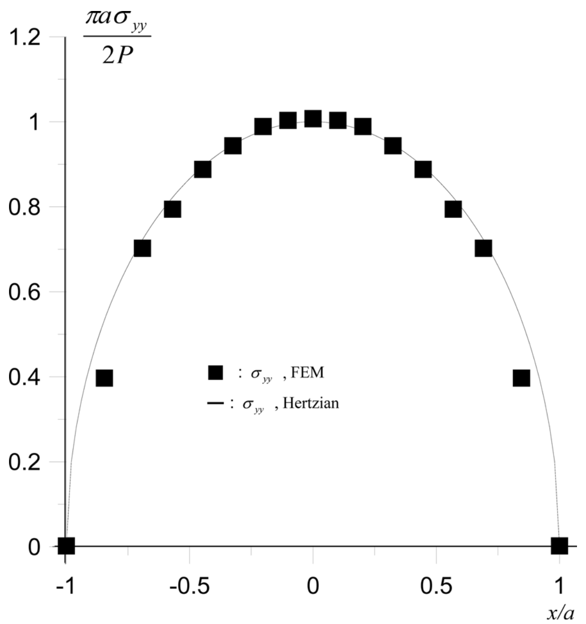

Fig. 6 Normal stress during frictionless contact between two elastically identical cylinders

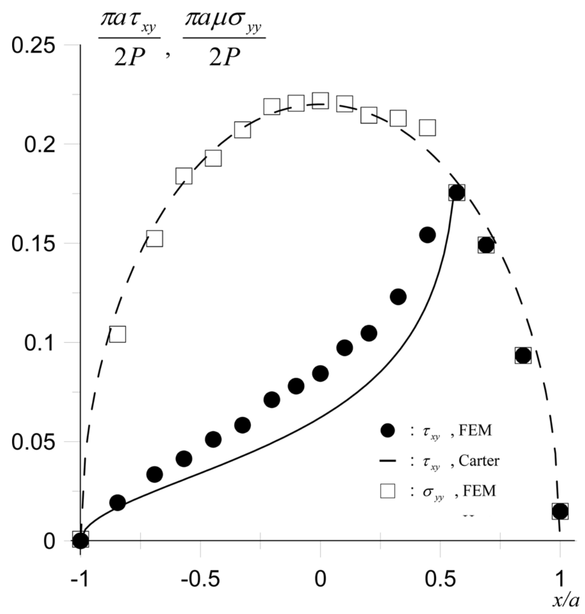

Fig. 7 Normal and shear stresses during rolling contact between two elastically identical cylinders; $\xi_x = -0.00029$, $Q/\mu P = 0.1875$

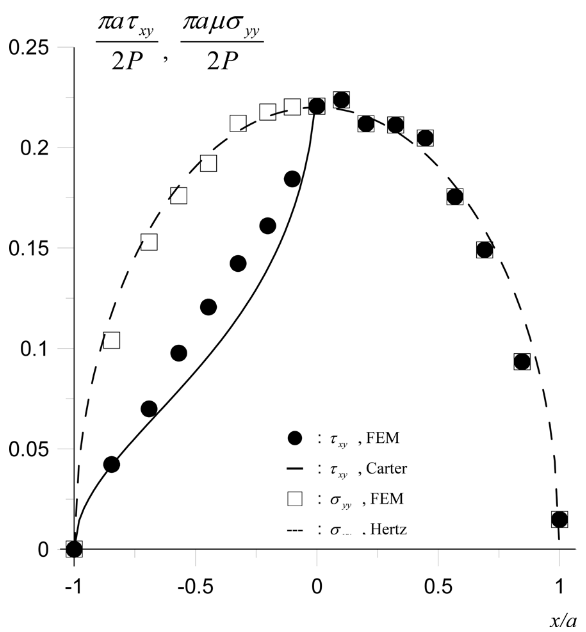

Fig. 8 Normal and shear stresses during rolling contact between two elastically identical cylinders; $\xi_x = -0.0007$, $Q/\mu P = 0.52$

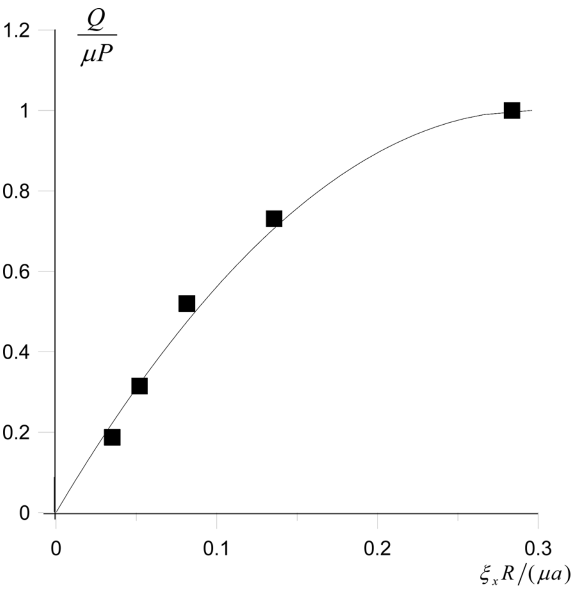

Fig. 9 The relation between force Q and longitudinal creep ratio ξ_x; R is half the radius of the two cylinders, solid ling is Carter's result

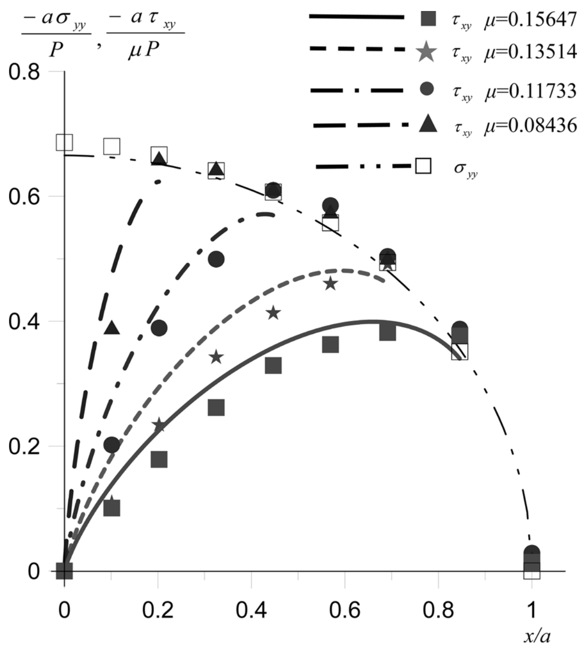

Fig. 10 Stresses in frictional normal contacts; results obtained by Nowell *et al.* (1988b) are denoted by various lines

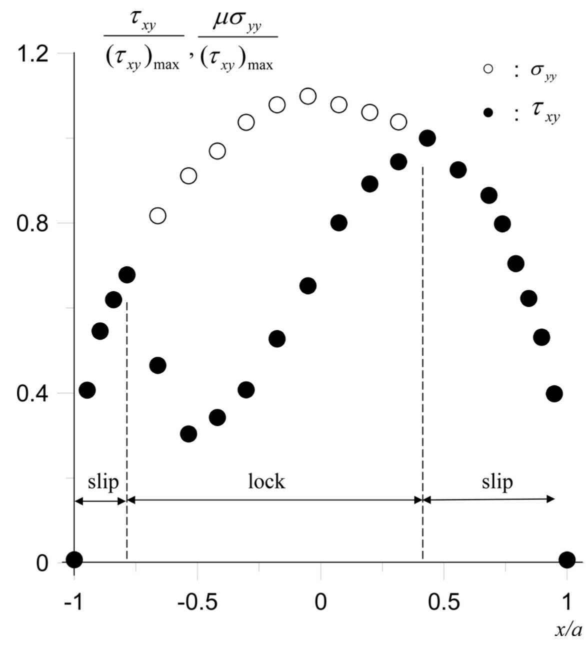

Fig. 11 Normal and shear stresses for rolling contact between two dissimilar materials; $\xi_x = -0.0158$, $Q/\mu P$ = 0.737, $\tau_{\max}$ = 421.6 MPa

of aluminum and steel, respectively. Fig. 10 shows the present solutions to normal contacts, compared to analytical results obtained by Nowell *et al.* (1988b). Note that in cases with elastic identical materials, the present solutions in shear stresses are somewhat higher than the analytic solutions, as Figs. 7 and 8 show. But in Fig. 10 the shear stresses are lower than corresponding analytical results. Perhaps the differences appear in Fig. 10 are due to the fact that the analytical solutions were obtained by neglecting the influence of tangential stress on the normal problem, while in the present solution this influence was not neglected.

Rolling contacts of dissimilar materials are discussed next. Although Eq. (21) is only valid for elastically identical materials, it is used, however, to estimate the critical value of creep ratio. In a state of gross sliding, $(Q/\mu P) = 1$, then Eq. (21) gives the corresponding creep ratio $\xi_x = -\mu a/R$. In the following analysis the initial contact size a = 4.717 mm. Hence the critical creep ratio to cause gross sliding is estimated to be −0.00637. Fig. 11 shows rolling contact results with the creep ratio $\xi_x = -0.0158$, about 2.5 times larger than the estimated critical value. Due to material dissimilarity, the two bodies still adheres to each other in more than half the contact region, as Fig. 11 shows. It can be seen that there exists two slip regions at the leading and the trailing edges. The same prescribed displacement Δy to obtain normal contact solutions is used in the rolling contact analysis, but an increase of the contact length from the normal contact solution can be observed. The results shown in Fig. 11 were obtained by specifying an increase in contact length to the right by one element at the outset of the analysis; it increases from the value a = 4.717 mm to the value a = 4.974 mm. Nowell and Hills (1988a) obtained semi-analytical solutions for rolling contact between dissimilar materials, and presented results for particular values of tangential forces. In the present analysis the value of the tangential force Q cannot be specified a priori; Q is the force that

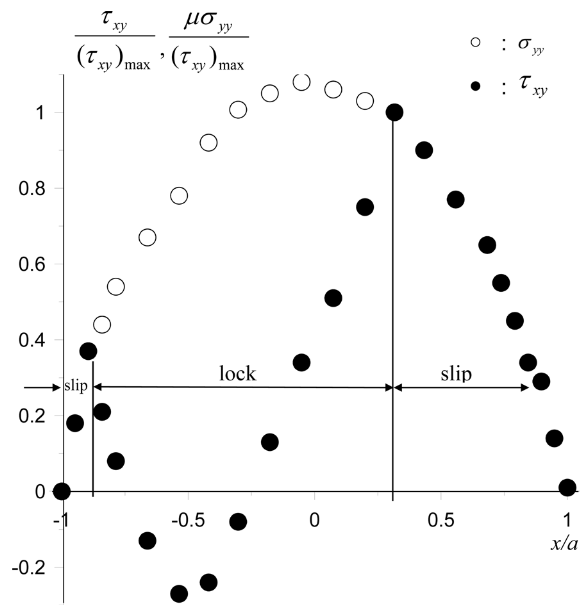

Fig. 12 Normal and shear stresses for tangential contact between two dissimilar materials, $\delta_x = -0.0032$ mm, $Q/\mu P = 0.514$, $\tau_{\max} = 409.7$ MPa

produces the prescribed change in the contact length, and the amount of this change in contact length can only be a multiple of an element length. Hence we are unable to compare the two solutions under the same situation, as we did in Fig. 10 for normal contact. However, we may observe that Nowell and Hills's results (1988a, Fig. 4(b)) also have two slip regions, they also appear at the leading and the trailing edges, and stress in the slip as well as in the stick regions have the same shapes as those shown in Fig. 11.

Fig. 12 shows tangential and normal stresses during a tangential contact with the rigid displacement $\delta_x = -0.0032$ mm. Tangential stress changes sign in a region of the stick zone, and this also appears in the solution obtained by Nowell *et al.* (1988b, Fig. 9(a)). As in the previous case, only solutions for particular values of δ_x and Q can be presented in this study; and these values are not the same as the values presented in Nowell *et al.* (1988b). Although a comparison in numerical values of the two solutions are unavailable at this stage, but the two solutions show the same distribution of the stick and the slip regions; and tangential stress curves in the two solutions have the same shape.

6. Conclusions

In this study a numerical technique is developed to deal with two dimensional normal, tangential, and rolling contact problems with or without friction and between identical or dissimilar materials. The idea is to express extrapolated stresses and strains in terms of nodal displacements, so that stress boundary conditions and kinematic conditions may be transformed into multiple constraints for nodal displacements. When these constraint equations are solved together with the finite element system equations, the nodal stresses and displacements satisfy all contact boundary conditions.

Solutions include the normal and the tangential stresses, and sizes of the stick and the slip regions. This method does not make use of nonlinear variational principles, nor does it require any special contact element.

Acknowledgements

The authors gratefully acknowledge the supported of the National Science Council of ROC under grant no. NSC92-2212-E-032-013.

References

Buscaglia, G.C., Durán, R., Fancello, E.A., Feijóo, R.A. and Padra, C. (2001), "An adaptive finite element approach for frictionless contact problems", *Int. J. Numer. Meth. Eng.*, **50**, 395-418.1

Carter, F.W. (1926), "On the action of a locomotive driving wheel", *Royal Society*, A112, 151.

Cerruti, V. (1882), Roma, Acc. Lincei, Mem fis. mat.

Cook, R.D., Malkus, D.S., Plesha, M.E. and Witt, R.J. (2001), *Concepts and Applications of Finite Element Analysis*, 4th Edition, John-Wiley.

Duvaut, G. and Lions, J.L. (1976), *Inequalities in Mechanics and Physics*, Springer, Berlin.

Eterovic, A.L. and Bathe, K.J. (1991), "On the treatment of inequality constraints arising from contact conditions in finite element analysis", *Comput. Struct.*, **40**, 203-209.

Ferronato, M., Janna, C. and Gambolati, G. (2008), "Mixed constraint preconditional contact mechanics", *Comput. Meth. Appl. Mech. Eng.*, **197**, 3922-3931.

González, J.A. and Abascal, R. (1998), "Using the boundary element method to solve rolling contact problems", *Eng. Anal. Bound. Elem.*, **21**(4), 385-392.

González, J.A., Park, K.C., Felippa, C.A. and Abascal, R. (2008), "A formulation based on localized lagrange multipliers for BEM-FEM coupling in contact problems", *Comput. Meth. Appl. Mech. Eng.*, **197**, 623-640.

Hassani, R., Hild, P., Ionescu, I.R. and Sakki, N.D. (2003), "A mixed finite element method and solution multiplicity for coulomb frictional contact", *Comput. Meth. Appl. Mech. Eng.*, **192**, 4517-4531.

Hedayatr, P., Azhari, M., Shahidi, A.R. and Bradford, M.A. (2007), "On the use of the Lagrange Multiplier Technique for the unilateral local buckling of point-restrained plates, with application to side-plated concrete beams in structural retrofit", *Struct. Eng. Mech.*, **26**(6), 673-685.

Hills, D.A., Nowell, D. and Sackfield, A. (1993), *Mechanics of Elastic Contacts*, Butterworth-Heinemann.

Hsu, J.Y. (1998), "Using constraint conditions for finite element analysis of two dimensional elastic contact problems with friction", Master Thesis, Department of Mechanical Engineering, Tamkang University, (in Chinese).

Johnson, K.L. (1958a), "The effect of spin upon the rolling motion of an elastic sphere on a plane", *J. Appl. Mech.*, **25**, 332-338.

Johnson, K.L. (1958b), "The effect of a tangential contact force upon the rolling motion of an elastic sphere on a plane", *J. Appl. Mech.*, **25**, 339-346.

Johnson, K.L. (1985), *Contact Mechanics*, Cambridge University Press, Cambridge, UK.

Kakoi, K. and Obara, T. (1993), "Numerical method for counterformal rolling contact problems using special boundary element method", *JSME Int. J.*, Series *A*, **36**(1), 57-62.

Kalker, J.J. (1967), "On the rolling contact of two elastic bodies in the presence of dry friction", Ph.D. Thesis, Delft University, 95-100.

Kalker, J.J. (1973), *Simplified Theory of Rolling Contact*, Delft Progress Report, Series C, 1-10.

Kalker, J.J. (1990), *Three-Dimensional Elastic Bodies in Rolling Contact*, Kluwer Academic Publishers, Delft, The Netherlands.

Kalker, J.J. (1991), "Wheel-rail rolling contact theory", *Wear*, **144**, 243-261.

Kikuchi, N. and Oden, J.T. (1988), *Contact Problems in Elasticity: A Study of Variational Inequalities and Finite Element Methods*, SIAM, Philadelphia.

Knothe, K., Wille, R. and Zastrau, B.W. (2001), "Advanced contact mechanics- road and rail", *Vehicle Syst. Dyn.,* **35(**4-5), 361-407.

Liu, C. and Paul, B. (1989), "Rolling contact with friction and non-hertzian pressure distribution", *J. Appl. Mech.*, **56(**4), 814-820.

Liu, C.H. and Hsu, J.Y. (2000), "Using constraint conditions for finite element analysis of two dimensional elastic contact problems with friction", *Proceedings of the European Congress on Computational Methods in Applied Sciences and Engineering*, Barcelona, September.

Mohamed, S.A., Helal, M.M. and Mahmoud, F.F. (2006), "An incremental convex programming model of the elastic frictional contact problems", *Struct. Eng. Mech.*, **23**(4), 431-447.

Nackenhorst, U. (2004), "The ALE-formulation of bodies in rolling contact theoretical foundations and finite element approach", *Comput. Meth. Appl. Mech. Eng.*, **193**, 4299-4322.

Nowell, D. and Hills, D.A. (1988a), "Tractive rolling of dissimilar elastic cylinders", *Int. J. Mech. Sci.*, **30**(6), 427-439.

Nowell, D., Hills, D.A. and Sackfield, A. (1988b), "Contact of dissimilar elastic cylinders under normal and tangential loading", *J. Mech. Phys. Solids*, **36**(1), 59-75.

Ozsahin, T.S. (2007), "Frictionless contact problem for a layer on an elastic half plane loaded by means of two dissimilar rigid punches", *Struct. Eng. Mech.*, **25**(4), 383-403.

Padovan, J. and Paramadilok, O. (1984), "Transient and steady state viscoelastic rolling contact", *Comput. Struct.*, **20**, 545-553.

Pauk, V. and Zastrau, B. (2003), "Rolling contact problem involving surface roughness", *Mech. Res. Commun.*, **30**, 45-51.

Paul, B. and Hashemi, J. (1981), "Contact pressures on closely conforming elastic bodies", *J. Appl. Mech.*, **48**, 543-548.

Solberg, J.M. and Papadopoulos, P. (2005), "An analysis of dual formulations for the finite element solution of two-body contact problems", *Comput. Meth. Appl. Mech. Eng.*, **194**, 2734-2780.

Solberg, J.M., Jones, R.E. and Papadopoulos, P. (2007), "A family of simple two-pass dual formulations for the finite element solution of contact problems", *Comput. Meth. Appl. Mech. Eng.*, **196**, 782-802.

Tallec, P.L. and Rahier, C. (1994), "Numerical methods of steady rolling for non-linear visco-elastic structures in finite deformations", *Int. J. Numer. Meth. Eng.,* **37**, 1159-1186.

Tsai, A.C. (2004), "Using Multiple Point Constraints in Finite Element Analysis of Two Dimensional Rolling Contact Between Dissimilar Materials", Master Thesis, Department of Mechanical and Electro-mechanical Engineering, Tamkang University, (in Chinese).

Wang, K.Y., Qin, Q.H., Kang, Y.L., Wang, J.S. and Qu, C.Y. (2005), "A direct constraint-trefftz FEM for analysing elastic contact problems", *Int. J. Numer. Meth. Eng.*, **63**, 1694-1718.

Wriggers, P. (2006), *Computational Contact Mechanics*, 2nd Edition, Springer, Berlin.